J. KSIAM Vol.21, No.4, 225–244, 2017 http://dx.doi.org/10.12941/jksiam.2017.21.225

# A NUMERICAL STUDY ON MHD NATURAL CONVECTIVE HEAT TRANSFER IN AN AG-WATER NANOFLUID FILLED ENCLOSURE WITH CENTER HEATER

N. NITHYADEVI AND T. MAHALAKSHMI†

DEPARTMENT OF MATHEMATICS, BHARATHIAR UNIVERSITY, COIMBATORE, TAMIL NADU, INDIA
*E-mail address*: saimaha13@gmail.com

ABSTRACT. The natural convective nanofluid flow and heat transfer inside a square enclosure with a center heater in the presence of magnetic field has been studied numerically. The vertical walls of the enclosure are cold and the top wall is adiabatic while the bottom wall is considered with constant heat source. The governing differential equations are solved by using a finite volume method based on SIMPLE algorithm. The parametric study is performed to analyze the effect of different lengths of center heater, Hartmann numbers and Rayleigh numbers. The heater effectiveness and temperature distribution are examined. The effect of all pertinent parameters on streamlines, isotherms, velocity profiles and average Nusselt numbers are presented. It is found that heat transfer increases with the increase of heater length, whereas it decreases with the increase of magnetic field effect. Furthermore, it is found that the value of Nusselt number depends strongly upon the Hartmann number for the increasing values of Rayleigh number.

## 1. INTRODUCTION

Natural convective heat transfer occurs in many engineering systems, such as power plant, home ventilation, fire prevention, reactor insulation, solar collectors, etc., [1]. Various aspects of natural convection heat transfer in enclosures have been investigated thoroughly by many researchers [2-6]. Transfer of heat from a localized heater inside an enclosure is considered in designing electronic devices and equipment cooling. An efficient cooling is essential for these electronic equipments. Therefore many researchers have investigated natural convection in enclosures with different types of heaters. Sun and Emery [7] examined conjugate heat transfer when the heater is located near the walls of enclosure with heat source both numerically and experimentally. Their results showed that for an enclosure with conductive heater, heat transfer was a function of heater conduction, fluid convection and strength of internal heating.

Oztop et al. [8] investigated the effect of position of a heater in an enclosure with cold vertical walls and adiabatic horizontal walls. They showed that more enhancements in heat transfer are obtained when the heated plate located vertically than horizontally. Ben-Nakhi and

Received by the editors August 5 2017; Accepted December 10 2017; Published online December 13 2017.
*Key words and phrases.* finite volume method; heat source; isothermal heater; magnetic field; nanofluid flow; natural convection.

† Corresponding author.

Chamkha [9] numerically analyzed the significant effect of thin heater inclination angle and heater length on natural convective fluid flow in a square enclosure. Their results showed that wall heat transfer enhancement or reduction was based on the appropriate selection of both heater inclination angle and length. Natural convection cooling of a horizontally attached heat source on the left adiabatic vertical wall of an enclosure filled with Cu-water nanofluid was numerically studied by Mahmoudi et al. [10]. They obtained that for the increasing length of the heater heat transfer decreases whereas it increases for increase in solid volume fraction of nanoparticles.

Stefanizzi et al. [11] carried out both experimental and numerical investigation of Heat Transfer in the Cavities of Hollow Blocks. They obtained the result that the thermal resistance of the cavity affects the overall thermal performance of the wall of hollow blocks significantly. Jani et al. [12] investigated natural convection heat transfer inside enclosure with high conductive vertical heater placed at the center of heated bottom wall. They observed the two different effects of heater that the first is the conductive heater increasing rate of heat transfer; the second is friction loss of heater weakens the fluid flow in the enclosure and which yield the decrease in heat transfer rate. Convective heat transfer inside a square enclosure having heat conducting and generating solid body has been analysed by Nithyadevi and Umadevi [13]. Their results showed that increase in heat transfer is obtained for sinusoidal heating with cold wall for increasing values of $\Delta T^*$ whereas for increasing thermal conductivity ratio heat transfer decreased for sinusoidal heating with cold wall.

Recently Ohk et al. [14] examined natural convection heat transfer in a vertical cylinder and obtained the results that for increasing diameter and length of pipe the heat transfer decreases. Very recently, Elater et al. [15] analyzed natural convection in a square enclosure with horizontal heater attached to its hot wall. They found that heater effectiveness enhanced with an increase of heater length. Currently, open square enclosure having diagonally placed heaters along with adiabatic square block filled with nanofluid has been considered by Kalidasan and Rajesh Khanna [16]. They found that significant heat transfer is reached for the location of heaters and heat transfer intensity is high at the right wall than the left wall of the enclosure. Esfe et al. [17] obtained the numerical results that enhancement in heat transfer is obtained by increasing solid volume fraction of nanofluid and reducing diameter of nanoparticles.

The influence of magnetic field on heat transfer had received considerable attention because in some practical cases such as crystal growth in fluids, cooling of nuclear reactor and petroleum industries natural convection happens under the influence of magnetic field. MHD flow and heat transfer phenomena induced by buoyancy and Lorentz force in enclosures was studied extensively in the literature [18-19]. Saha [20] investigated numerically the steady magneto-convection in a sinusoidal corrugated enclosure with constant heat flux source discretely embedded at the bottom wall. His results indicated that when the heat source surface area increases, the rate of heat transfer also increases and the heat source size and magnetic field has significant effect on the heat transfer rate.

The magneto convection in a tilted square enclosure with differentially thermally active vertical walls was studied numerically by Subbarayalu and Velappan [21]. Their results showed that the heat transfer increases with increase of Grashof number but decreases with increase of

magnetic field effect and behaves in a non-linear fashion with angles of inclination. Recently, natural convection inside the L-shaped enclosure in the presence of a magnetic field was analyzed numerically by Sourtiji and Hosseinizadeh [22]. Their results showed that performance of nanofluid utilization is more effective at high Rayleigh numbers and heat transfer increases with increasing solid volume fraction of nanofluid. Also they found that increasing effect of magnetic field yield the significant decrease in overall heat transfer. Bakhshan and Ashoori [23] investigated a natural convection in a rectangular enclosure filled with an electrically conducting fluid. They observed that heat transfer decreases with increasing effect of magnetic field.

Ali Al-Zamily [24] numerically investigated natural convection in a semicircular enclosure filled with Cu-water nanofluid with bottom heat flux. He found that effect of magnetic field on heat transfer decreases with increase of nanoparticles fraction effect. Ben-hamida and Charrada [25] also obtained similar result by considering enclosure filled with an ethylene glycol copper nanofluid under the effect of magnetic field. Javaherdeh et al. [26] has performed the analysis on magneto hydrodynamic nanofluid flow in wavy enclosure. The results of their study indicated that increasing nanoparticles concentration enhances heat transfer rate. Meanwhile heat transfer rate decreases for increasing the effect of magnetic field.

In recent years, nanofluids that are a suspension of nano-sized solid particles in a base fluid with higher thermal conductivity than the based fluid which are used to enhance the rate of heat transfer in many applications [27-31]. Ogut [32] examined numerically the natural convection of water-based nanofluids in an inclined square enclosure with a constant heat flux at the center of its left wall. He obtained the results that the average heat transfer rate increases significantly as nanoparticle volume fraction increased. Also his results showed that flow and temperature fields are affected by length of the heater. The natural convection in a square enclosure filled with both $Al_2O_3$ -water and the CuO-water nanofluids was analyzed by Abu-nada et al. [33] considering temperature dependent viscosity, thermal conductivity relationships and volume fraction of nanoparticles.

Ghasemi et al. [34] investigated numerically the natural convection flow in an enclosure filled with $Al_2O_3$ nanofluid under the influence of horizontally applied magnetic field and obtained that heat transfer rate increases or decreases as solid volume fraction of nanoparticles increases depending on the Hartmann number. Sheikhaleslami and Gorji-Bandpy [35] utilized Lattice Boltzmann method to investigate ferrofluid flow and heat transfer inside the enclosure in the presence of external magnetic source. Their results showed that heat transfer increases with increase of Rayleigh number and heat source length but it decreases with increase of size of nanoparticles. Selimefendigil et al. [36] studied natural convection and entropy generation entrapped trapezoidal enclosure filled with nanofluid under magnetic field effect. They found that heat transfer increased for increasing volume fraction of a nanoparticle. Also their results showed that even for higher values of Rayleigh number, reduction of heat transfer by the magnetic field effect was more pronounced.

Based on the above literature reviews, despite numerous studies on natural convection of nanofluids inside enclosures with different heat sources, there is no study on natural convection inside the square enclosure with center heater under the effect of magnetic field utilizing

Ag-water nanofluid. In the present study the problem of natural convection heat transfer and nanofluid flow in a square enclosure is investigated for different length of inside thin heater with bottom heat source in the presence of magnetic field. This innovative technique could be utilized to enhance heat transfer in cooling of electronic devices equipped with nanofluids, heat exchangers, energy storage systems, food processing and lubrication technologies.

## 2. MATHEMATICAL FORMULATION

The configuration of the square enclosure considered in this present study is shown in Figure 1. The height and width of the enclosure are denoted by L. Two side walls are maintained at a constant cold temperature $T_c$ whereas the bottom wall is considered with heat source of fixed length. The remaining parts of bottom and top walls are kept adiabatic. A thin heater with temperature $T_h$ is located in the centre of the enclosure at both horizontal and vertical positions. The length of the heater is denoted by $\Gamma$. Also uniform and constant magnetic field of strength $B_0$ is applied longitudinally. The working fluid employed in this enclosure is water based nanofluid containing Ag nanoparticles which is assumed to be Newtonian and incompressible. It is assumed that both base fluid and nanoparticles are in thermal equilibrium. Except for the density variation, properties of base fluid and nanoparticles are assumed to be constant. The thermo physical properties of the water and the silver (Ag) nanoparticles are given in Table1.

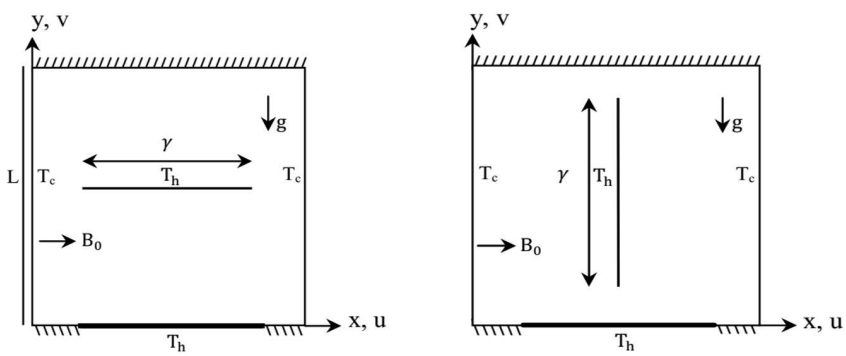


FIGURE 1. Configuration of the problem

The continuity, momentum and energy equations for two dimensional problem of steady state laminar natural convection in an enclosure are:

$$\frac{\partial u}{\partial x}+\frac{\partial v}{\partial y}=0 \tag{2.1}$$

$$\mathrm{u}\frac{\partial u}{\partial x}+v\frac{\partial u}{\partial y}=-\frac{1}{\rho_{nf}}\frac{\partial \rho}{\partial x}+\frac{\mu_{nf}}{\rho_{nf}}\nabla^2 u \tag{2.2}$$

$$u\frac{\partial v}{\partial x}+v\frac{\partial v}{\partial y}=-\frac{1}{\rho_{nf}}\frac{\partial \rho}{\partial y}+\frac{\mu_{nf}}{\rho_{nf}}\nabla^2 v+\frac{(\rho\beta)_{nf}}{\rho_{nf}}g\left(T-T_c\right)-\frac{\sigma_{nf}}{\rho_{nf}}B_o^2 v \tag{2.3}$$

and

$$u\frac{\partial T}{\partial x}+v\frac{\partial T}{\partial y}=\alpha_{nf}\left(\nabla^2 T\right) \tag{2.4}$$

The boundary conditions for Eqs. (2.1)–(2.4) are:

$$\begin{aligned}
&u=v=0, \quad T=T_c \quad at \quad x=0, \quad L \quad and \quad 0\leq y\leq L\\
&u=v=0, \quad \frac{\partial T}{\partial y}=0 \quad at \quad y=0, \quad 0\leq x<\frac{L-l}{2}, \frac{L+l}{2}<x\leq L\\
&u=v=0, \quad T=1 \quad at \quad y=0, \quad \frac{L-l}{2}\leq x\leq\frac{L+l}{2}\\
&u=v=0, \quad \frac{\partial T}{\partial y}=0 \quad at \quad y=L\,,\ 0\leq x\leq L
\end{aligned} \tag{2.5}$$

and on the heater

$$u=v=0, \quad T=T_h$$

where the effective density and heat capacity of the nanofluid are calculated from the following equations:

$$\rho_{nf}=(1-\varphi)\,\rho_f+\varphi\rho_s \tag{2.6}$$

TABLE 1. Thermophysical properties of base fluid and solid nanoparticles

| Physical properties | Fluid phase(water) | Solid phase(Ag) |
|---|---|---|
| $C_p$(J/kg/K) | 4179 | 235 |
| $\rho$(kg/m$^3$) | 997.1 | 10,500 |
| k(W/mk) | 0.613 | 429 |
| $\beta$x10$^5$(k$^{-1}$) | 21 | 1.89 |
| $\sigma$x10$^7$(S/m) | 0.05 | 6.30 |

Under the thermal equilibrium conditions the specific heat of nanofluid is given as

$$(\rho_{cp})_{nf}=(1-\varphi)\,(\rho_{cp})_f+\varphi\left(\rho c_p\right)_s \tag{2.7}$$

The thermal expansion coefficient of the nanofluid can be obtained from

$$(\rho\beta)_{nf}=(1-\varphi)\,(\rho\beta)_f+\varphi\,(\rho\beta)_s \tag{2.8}$$

The thermal diffusivity of the nanofluid is

$$\alpha_{nf}=\frac{k_{nf}}{(\rho_{cp})_{nf}} \tag{2.9}$$

In this study, the Brinkman model is used for the viscosity of the nanofluid. So the effective dynamic viscosity of the nanofluid is obtained from the formula

$$\mu_{nf}=\mu_f(1-\varphi)^{-2.5} \tag{2.10}$$

The effective thermal conductivity of the nanofluid is determined by using the Maxwell model. For the suspension of spherical nanoparticles in the base fluid, it is written as:

$$\frac{k_{nf}}{k_f}=\frac{(k_f+2k_f)-2\varphi\,(k_f-k_s)}{(k_f+2k_s)+\varphi\,(k_f-k_s)} \tag{2.11}$$

Also the electrical conductivity of the nanofluid is given as:

$$\sigma_{nf}=(1-\varphi)\,\sigma_f+\varphi\sigma_s \tag{2.12}$$

Using the following dimensionless parameters, the governing equations can be converted to dimensionless forms

$$X=\frac{x}{L},\quad Y=\frac{y}{L},\quad U=\frac{uL}{\alpha_f},\quad V=\frac{vL}{\alpha_f},\quad P=\frac{pL^2}{\rho_{nf}\,\alpha_f^2},\quad \theta=\frac{T-T_c}{T_h-T_c},$$

$$Pr=\frac{\nu_f}{\alpha_f}\,,\ Ra=\frac{g\beta_f\,(T_h-T_c)\,L^3}{\alpha_f\nu_f},\ Ha=B_0L\sqrt{\sigma_{nf}/\rho_{nf}\nu_f} \tag{2.13}$$

By using the above dimensionless variables, the governing equations (2.1)–(2.4) in dimensionless forms are as follows:

$$\frac{\partial U}{\partial X}+\frac{\partial V}{\partial Y}=0 \tag{2.14}$$

$$U\frac{\partial U}{\partial X}+V\frac{\partial U}{\partial Y}=-\frac{\partial P}{\partial X}+\frac{\mu_{nf}}{\rho_{nf}\alpha_f}\nabla^2U \tag{2.15}$$

$$U\frac{\partial V}{\partial X}+V\frac{\partial V}{\partial Y}=-\frac{\partial P}{\partial Y}+\frac{\mu_{nf}}{\rho_{nf}\alpha_f}\nabla^2V+\frac{(\rho\beta)_{nf}}{\rho_{nf}\beta_f}RaPr\theta-Ha^2PrV \tag{2.16}$$

$$U\frac{\partial \theta}{\partial X}+V\frac{\partial \theta}{\partial Y}=\frac{\alpha_{nf}}{\alpha_f}\nabla^2\theta \tag{2.17}$$

The boundary conditions for equations (2.14)–(2.17) are:

$$\begin{aligned}
&U=V=0,\quad \theta=0\quad at\quad X=0,\,1\quad and\quad 0\le Y\le 1\\
&U=V=0,\quad \frac{\partial\theta}{\partial Y}=0\quad at\quad Y=0,\,0\le X<\frac{1-\varepsilon}{2}\,,\,\frac{1+\varepsilon}{2}<X\le 1\\
&U=V=0,\quad \theta=1\quad at\quad Y=0\quad and\quad \frac{1-\varepsilon}{2}\le X\le\frac{1+\varepsilon}{2}\\
&U=V=0,\quad \frac{\partial\theta}{\partial Y}=0\quad at\quad Y=1\quad and\quad 0\le X\le 1
\end{aligned} \tag{2.18}$$

and on the heater

$$u=v=0,\quad \theta=1$$

The local Nusselt number along the vertical walls of an enclosure can be written as:

$$Nu\,(Y)=-\frac{k_{nf}}{k_f}\left(\frac{\partial\theta}{\partial X}\right)_{X=0,1}$$

The average Nusselt number is calculated by integrating the local Nusselt number along the vertical walls

$$\bar{Nu}\left(Y\right)=\frac{1}{2}\left[\left(\int_{0}^{1}Nu\left(Y\right)\left(dY\right)_{X=0}\right)+\left(\int_{0}^{1}Nu\left(Y\right)\left(dY\right)_{X=1}\right)\right]$$

For the bottom wall:

$$\bar{Nu}\left(X\right)=\int_{\frac{1-\varepsilon}{2}}^{\frac{1+\varepsilon}{2}}Nu\left(X\right)dX$$

$\varepsilon$ is length of bottom heat source.

## 3. Numerical approach and code validation

3.1. **Method of Solution.** The non dimensional governing equations (2.14)–(2.17) subject to the boundary conditions are integrated over a finite volume method and solved numerically by the SIMPLE algorithm of Patankar [37] for the treatment of the pressure-velocity coupling together with under relaxation technique. The power law scheme is applied for convective terms and central difference scheme is applied for diffusion terms. The resulting sets of discreet algebraic equations for each variable are solved by a line-by-line procedure, combining the tri-diagonal matrix algorithm (TDMA). The convergence of the numerical results is established at each time step until a steady state is reached. The convergence condition used for this study is:

$$\left|\frac{\varphi_{n+1}\left(i,j\right)-\varphi_{n}(i,j)}{\varphi_{n+1}\left(i,j\right)}\right|\leq10^{-5}$$

where $\varphi$ represents the variables $U$, $V$ and $T$. The index $n+1$ is the current calculation and n denotes the previous calculation in the iteration, here $(i,j)$ refers to the space coordinates.

3.2. **Code Validation and Comparison with Previous Research.** To confirm the grid independence of the solution scheme, different grid size ranging from $21\times21$ to $141\times141$ (See Table 2) were used. The present developed FORTRAN code is tested for grid independence by calculating the average Nusselt number on the side walls. The significant changes occur in the average Nusselt number, for grid size varies from $21\times21$ to $121\times121$ and for grid size $121\times121$ to $141\times141$ the average Nusselt number for all cases remains unchanged. Hence, it is found that a uniform grid size of $121\times121$ ensure the grid independence for the present computations which was found to be sufficient to reach the steady solution for the Ag - Water nanofluid with $\varphi=0.06$. The present numerical solution is validated by direct comparisons against the results of Mahmoodi [38] for heat transfer in square enclosure with center heater filled with pure water at $Ra=10^{3}$ to $10^{6}$ which is shown in Figure 2.

Another validation test was carried out for comparison of present numerical result with those obtained by Ghasemi et al. [34] for natural convection in an enclosure filled with Water - $Al_2O_3$ nanofluid for Hartmann number $Ha=30$, different Rayleigh numbers and different solid volume fractions $\varphi$ of nanofluid is shown in Table 3. All these favorable comparisons lend confidence in the numerical results to be reported in the next section.

TABLE 2. Grid independence Test for vertical heater of length $\Gamma = 0.5$, $Ra = 10^4$, $\epsilon = 0.8$ and $\varphi = 0.06$.

| Grid size | $\overline{Nu}$ | Error % |
|---|---|---|
| $21 \times 21$ | 3.093351 | 13.16 |
| $41 \times 41$ | 3.562338 | 2.050 |
| $61 \times 61$ | 3.636895 | 0.668 |
| $81 \times 81$ | 3.661375 | 0.292 |
| $101 \times 101$ | 3.672102 | 0.124 |
| $121 \times 121$ | 3.676670 | 0.002 |
| $141 \times 141$ | 3.676780 | |

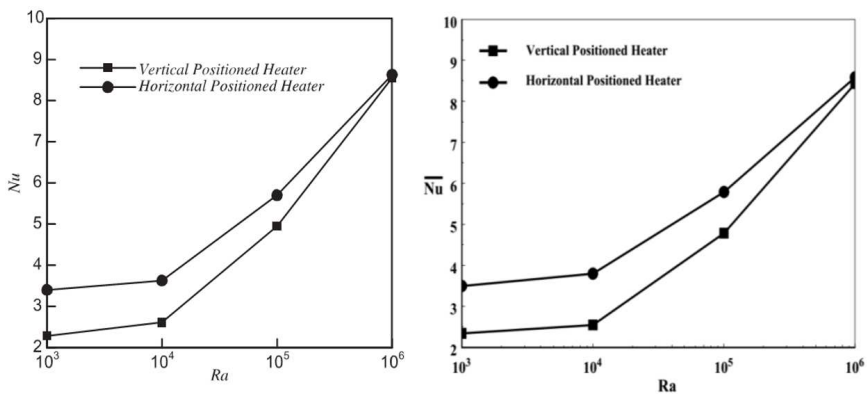


FIGURE 2. Comparison of present results with Mahmoodi [38]

## 4. RESULTS AND DISCUSSION

In this section, results are presented to illustrate the effects of various controlling parameters on the fluid flow and heat transfer processes inside the enclosure filled with Ag-water nanofluid. These controlling parameters include Hartmann number, three different length of horizontal, vertical heater and bottom heat source with fixed length $\epsilon = 0.8$. The influence of the magnetic field ($Ha = 0, 25, 50$) on the flow patterns and isotherms inside the enclosure at $Ra = 10^5$, $10^6$ and $10^7$ for different length of center heater ($\Gamma = 0.25, 0.5$ and $0.75$) are shown in Figs 3 to 8.

For all cases, the buoyancy forces generated due to the fluid temperature differences. The hot fluid over the bottom heat source rises from the middle portion of the bottom wall to the side cold walls. The rising hot fluid that gets blocked at the top adiabatic wall, which turns the flow and then descends downwards and turns back to the central region after hitting the bottom wall. This processing creates two symmetrical cells in the left and right halves of the enclosure with

TABLE 3. Comparison of average Nusselt number for different Rayleigh numbers and $\varphi$ for $Ha = 30$.

| Ra | $\varphi$ | $Nu$ | Present Study |
|---|---|---|---|
| | | Ghasemi et al.[34] | |
| $10^3$ | 0 | 1.002 | 1.045249 |
| | 0.02 | 1.060 | 1.049591 |
| | 0.04 | 1.121 | 1.108222 |
| | 0.06 | 1.184 | 1.154937 |
| $10^4$ | 0 | 1.183 | 1.175236 |
| | 0.02 | 1.212 | 1.193954 |
| | 0.04 | 1.249 | 1.189233 |
| | 0.06 | 1.291 | 1.238562 |
| $10^5$ | 0 | 3.150 | 3.096256 |
| | 0.02 | 3.138 | 3.087560 |
| | 0.04 | 3.124 | 3.080359 |
| | 0.06 | 3.108 | 3.089125 |
| $10^6$ | 0 | 7.907 | 7.895364 |
| | 0.02 | 7.979 | 7.928563 |
| | 0.04 | 8.042 | 8.019586 |
| | 0.06 | 8.098 | 8.045284 |

anticlockwise and clockwise rotations respectively due to the symmetrical boundary conditions at the vertical walls.

Figure 3 shows the streamlines and isotherms inside the enclosure with center horizontal heater with $\Gamma = 0.5$ for the strength of magnetic field with $Ha = 0, 25, 50$, $Ra = 10^5$, $10^6$ and $10^7$. It is evident from this figure that in the absence of magnetic field, by increasing Rayleigh number, the flow becomes stronger as natural convection is intensified by the increasing buoyancy force. At $Ra = 10^6$ and $10^7$, the nanofluid flow under the heater gets more strengthened than over the heater. At $Ra = 10^7$, the inner cells over and under the heater at both right and left sides of the enclosure coalesce and two more inner eddies with high flow rate are formed in the cell below the heater. Their isotherms show how the dominant heat transfer mechanism changes as Rayleigh number increases. Also for all Rayleigh numbers, by applying the magnetic field natural convection has been suppressed so that the fluid velocity decreases and dampens the heat transfer (the buoyancy force decreases). As the Hartmann number increases, the conduction heat transfer is dominating the flow inside the enclosure and the shape of the streamline tends to compress for all increasing Rayleigh number.

The stratification of the temperature field inside the enclosure begins to diminish as Hartmann number increases and the isotherms are almost parallel to the vertical walls indicating the occurrence of heat transfer is by heat conduction. As the effect of Hartmann number on

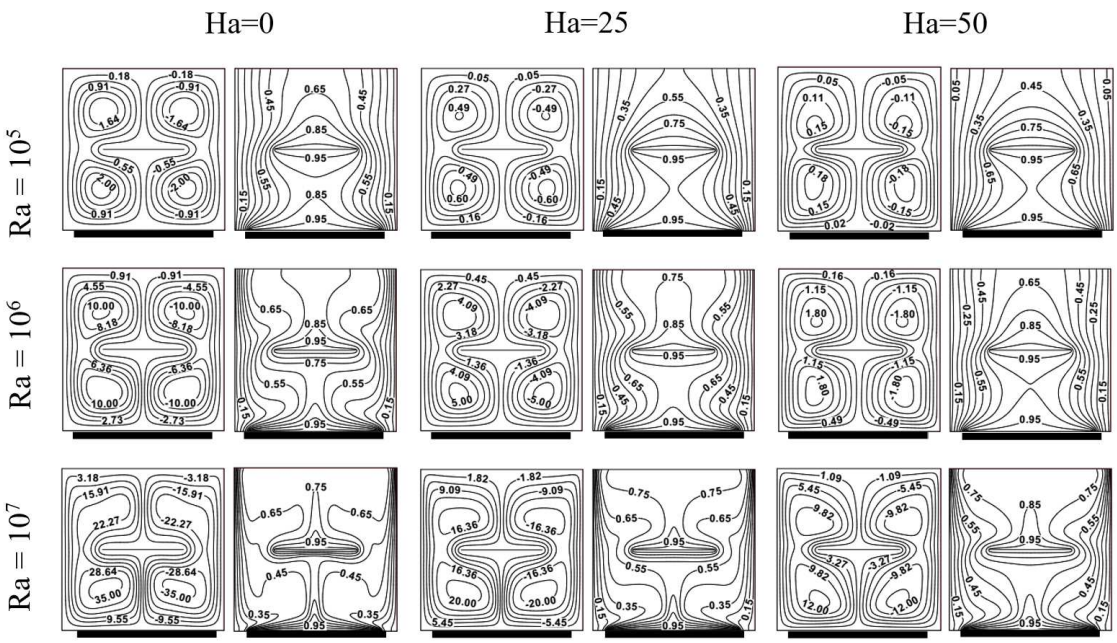


FIGURE 3. Streamlines and isotherms inside the enclosure filled with Ag-water nanofluid for horizontal positioned heater with length $\Gamma = 0.5$ at different Rayleigh numbers and Hartmann numbers

the nanofluid is high, even though the heater length is $\Gamma = 0.5$ the heat transfers by convection damps due to reducing fluid velocity. This is clearly seen from the reducing flow rate on streamline for increasing Ha values. The corresponding temperature contours shows that the thermal boundary layers at the two side walls disappear accordingly.

Figure 4 illustrates the streamlines and isotherms for different horizontal heater length and increasing Ha values at $Ra = 10^6$. In the absence of magnetic field ($Ha = 0$) at $\Gamma = 0.25$, here exist strong inner rotating cells below the center heater in the main recirculating cells. When heater length is increased to $\Gamma = 0.5$, two more inner cells above the heater exist and the entire recirculating cells become more strengthen for the maximum heater length $\Gamma = 0.75$. Moreover, the maximum heater length $\Gamma = 0.75$ separates the two recirculating cells in to four individual rotating cells. Similar trend can also be seen for $ha = 25$ with decreasing convection. For the maximum Hartmann value $Ha = 50$, these rotating cells become weaker as it is clearly seen from their flow rate and the main recirculating cells lose their strength. The corresponding isotherms seem to be very close around the heater and above the bottom heat source for $ha = 0$ and this trend becomes weak for increasing Hartmann values for all length of heater. The effect of magnetic field changes the mode of heat transfers from convection to conduction as expected which can be observed from the corresponding isotherms parallel to the vertical walls.

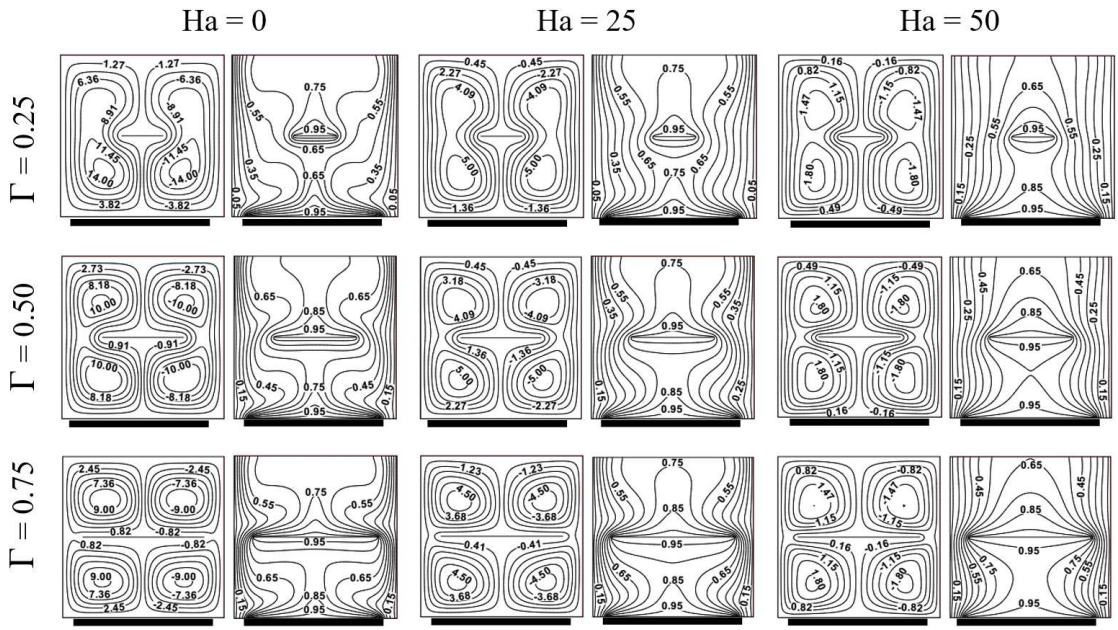


FIGURE 4. Streamlines and isotherms inside the enclosure filled with Ag-water nanofluid for horizontal positioned heater with different length for different Hartmann number at Ra $= 10^6$

The effects of Rayleigh number on streamlines and isotherms for horizontal heater of different length $\Gamma = 0.25, 0.5, 0.75$ at $Ha = 25$ are depicted in Figure 5. Generally, Rayleigh number effect on the nanofluid enhances the fluid velocity which in turn increases the buoyancy force and convection heat transfer becomes stronger. The existing inner cells below the center heater of length $\Gamma = 0.25$ at $Ra = 10^5$ get strengthen for further increasing Ra values. But for $\Gamma = 0.5$ more fluid flow is seen in the core above the heater becomes stronger for $Ra = 10^6$ and $10^7$. Similar trend can also be seen for $\Gamma = 0.75$ and is important to notice that at $Ra = 10^7$ and $\Gamma = 0.75$ the shape of central region of cells which are elliptical in shape above and below the heater confirms the occurrence of stronger convection heat transfer. The variation of isotherms with respect to Rayleigh numbers and heater lengths show that for all values of $\Gamma$ at $Ra = 10^5$ convection heat transfer is low and with increase in Ra values it turns into stronger as expected. It is clearly seen from the isotherms that occurrence of thermal stratification below the center heater also becomes stronger for increasing heater length. This is due to the high fluid moment and heat transfer inside the enclosure occurs totally by convection. Moreover, the existing thermal plum above the heater and bottom heat source shows the expected high heat transfer is obtained for the maximum heater length.

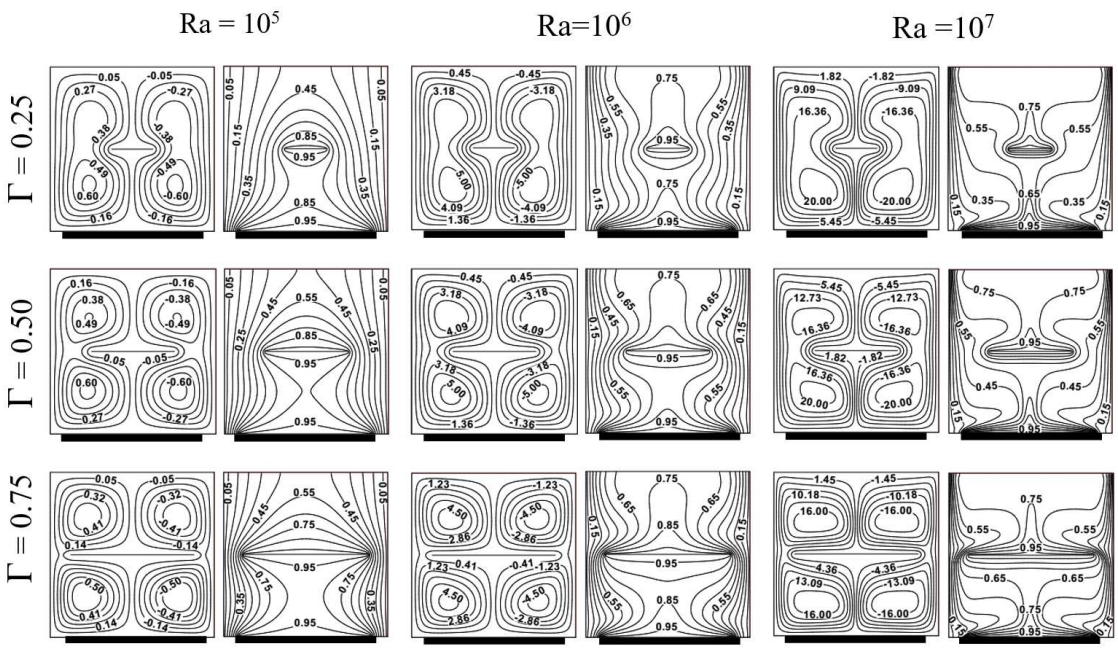


FIGURE 5. Streamlines and isotherms inside the enclosure filled with Ag-water nanofluid for horizontal positioned heater with different length for different Rayleigh numbers at $Ha = 25$

The influence of magnetic field (Ha) on the flow patterns and isotherms inside the enclosure with vertical heater of length $\Gamma = 0.5$ at $Ra = 10^5 - 10^7$ is shown in Figure 6. As Hartmann number effect on the nanofluid damps the fluid velocity causes the decrease of buoyancy force and convection heat transfer decreased. In the absence of magnetic field ($Ha = 0$), the two counter rotating cells at left and right side of center vertical heater occupies the maximum portion of enclosure rotates with high intensity at $Ra = 10^6$ and the shape of central region cell changes significantly for $Ra = 10^7$. It is evident that the isotherms are densely packed around the heater and above the bottom heat source for increasing Rayleigh number. It is clearly seen that occurrence of thermal stratification at two side of vertical heater also becomes stronger for increasing Rayleigh number. This is due to the high fluid flow and heat transfer inside the enclosure occurs totally by convection. But at $Ha = 25$ and $Ra = 10^5$, the main cells lose its strength as the fluid velocity decreases and when Ha increases further ($Ha = 50$) its flow intensity completely weaken. When $Ra = 10^6$ the streamlines are deformed and elongated more vertically for increment of Ha numbers from 25 to 50 and the circulation in the flow pattern is progressively restricted to the entire region. Since the applied magnetic field has the tendency to slow down the movement of the fluid in the enclosure, the flow circulation inhibits gradually and the flow at the core region becomes almost stagnant for $Ra = 10^7$. It is clearly seen from their isotherms that the heat distribution decreases as the strength of

magnetic field increases. In particular, a considerable decrease in heat transfer is achieved for higher Hartmann number.

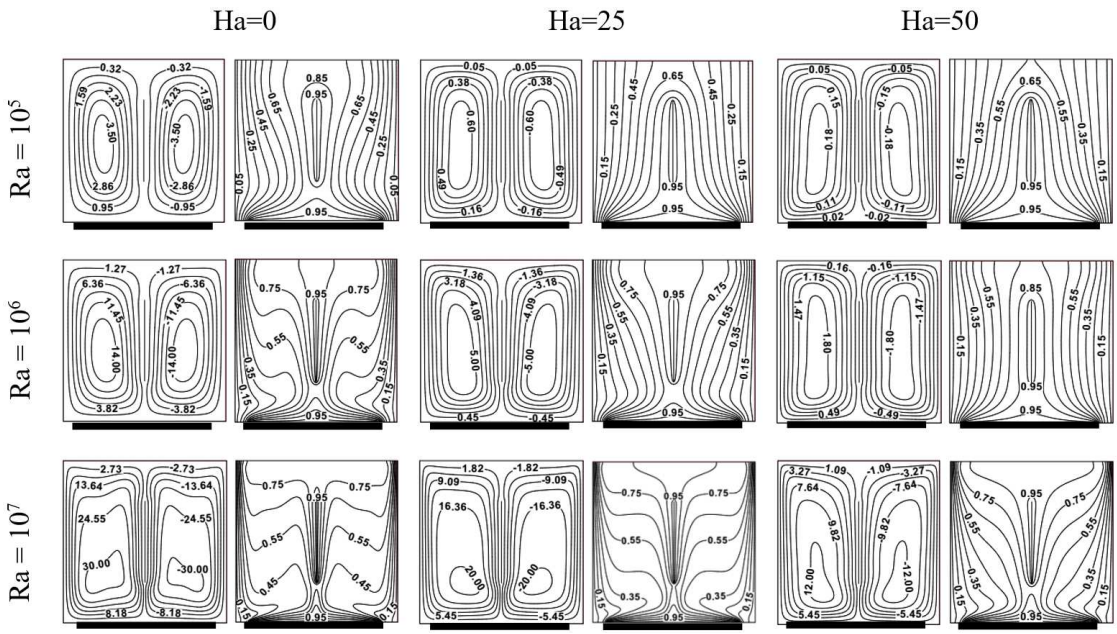


FIGURE 6. Streamlines and isotherms inside the enclosure filled with Ag-water nanofluid for vertical positioned heater with length $\Gamma = 0.5$ at different Rayleigh numbers and Hartmann numbers

Figure 7 illustrates the streamline and isotherm pattern for different length of vertical heater and Hartmann numbers ($Ha = 0, 25, 50$) at $Ra = 10^6$. The fluid flow is described by two major circulating cells occupying the entire enclosure. It is also observed that there exists a circulating flow of elliptical shape in the core of the enclosure and when Ha increased to 25 and 50, their shapes change significantly. The corresponding isotherms confirm that the temperature of the fluid decreases for increasing Ha numbers which affect the heat transfer characteristic inside the enclosure.

Because of the symmetrical condition about vertical walls, the isotherms are symmetrical at the vertical center line of the enclosure. The isotherms value decreases as the Hartmann number increases due to the decrease of the fluid movement. The higher temperature value appears near the center of the heater decreases towards the heat source edges with the increase of Hartmann number, the isotherms shapes changes from curved to less curved.

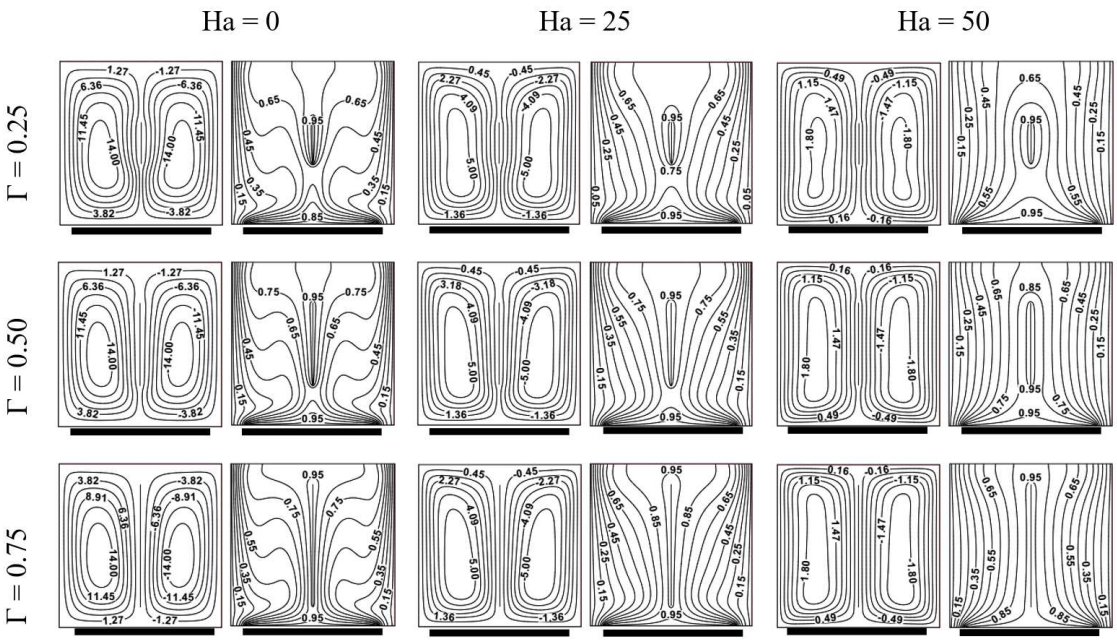


FIGURE 7. Streamlines and isotherms inside the enclosure filled with Ag-water nanofluid for vertical positioned heater with different length for different Hartmann number at Ra $= 10^6$

The influence of Rayleigh number (Ra) on the flow patterns and isotherms inside the enclosure for different vertical heater length at $Ha = 25$ is shown in Figure 8. The two major rotating vertices appear in the streamline pattern for all range of Rayleigh numbers and heater length. But when Ra increased from $10^5$ to $10^6$ at $\Gamma = 0.25$ its strength increases and for $Ra = 10^7$ two more inner vortices with high flow rate in the bottom of core above the heat source exists as the buoyancy force is high. For further increase in heater length, the cells in core region spans more vertically in the main two cells which shows the occurrence of complete convection in the enclosure. It is clearly shown from the isotherms that the temperature gradient around the increasing length of heater increases as the Rayleigh number increases. The temperature gradients adjacent to the walls are also increases which confirm the enhanced convection mechanism. The cell center shows affluent motion of active fluid at core region, their corresponding isotherms show heat transfer in the enclosure is controlled mainly by convection for all increasing values of Rayleigh number and heater length.

The suppression of the velocity field by the magnetic field effect is demonstrated in Figures 9 and 10 by the mid height vertical velocities for different values of Ha, horizontal and vertical heater respectively. From these figures we observe that the velocity field is considerably decreased for the increasing effect of magnetic field. The velocity profiles are flattened for higher values of the Hartmann number. It is also observed that the fluid particle moves with greater velocity for the low values of Hartmann number whereas the velocity is very lower for high

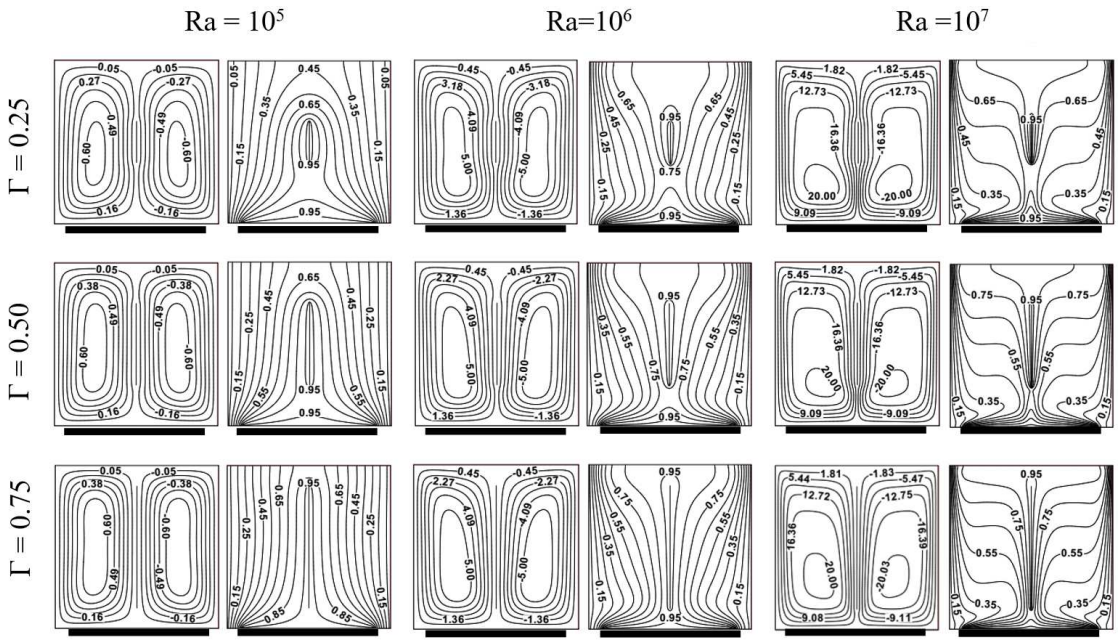


FIGURE 8. Streamlines and isotherms inside the enclosure filled with Ag-water nanofluid for vertical positioned heater with different length for different Rayleigh numbers at $Ha = 25$

values of Hartmann number. When comparing the velocity profiles in Figures 9 and 10, the considerable enhanced velocity field is observed in Figure 10 because of the obtained high heat transfer for the vertical heater compared with horizontal heater is maximum.

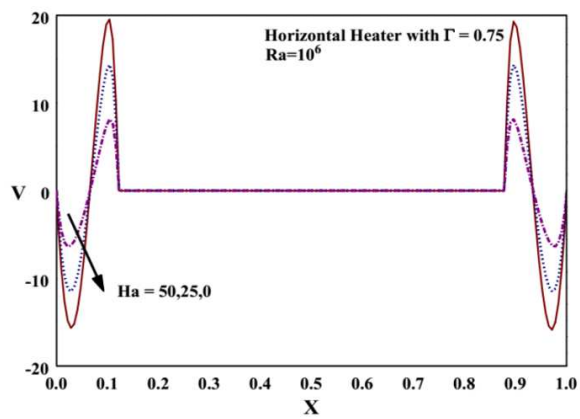


FIGURE 9. Mid height vertical velocity at the middle of the enclosure for horizontal heater ($\Gamma = 0.75$), different Hartmann numbers at $Ra = 10^6$

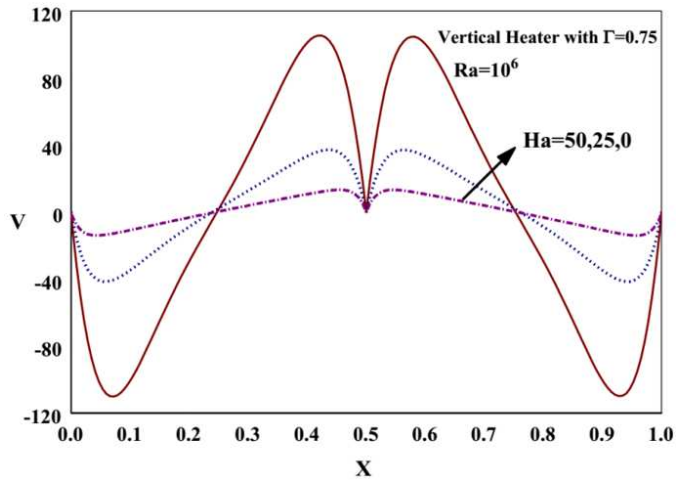


FIGURE 10. Mid height vertical velocity at the middle of the enclosure for vertical heater ($\Gamma = 0.75$), different Hartmann numbers at $Ra = 10^6$

Overall heat transfer in terms of average Nusselt number for different length of both horizontal and vertical heaters are depicted in Figure 11 for different Hartmann numbers.

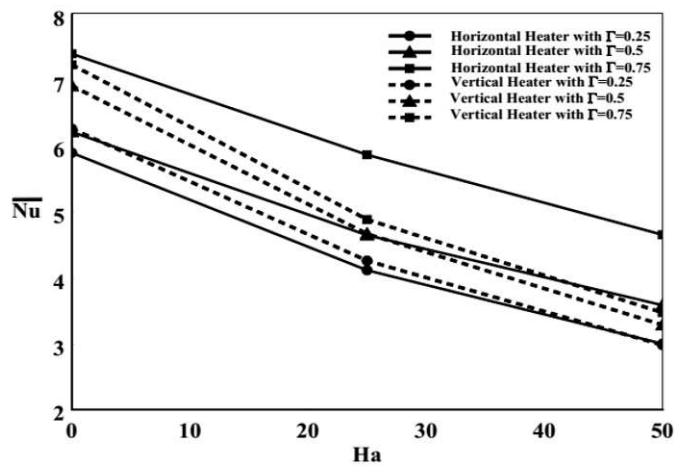


FIGURE 11. Variation of average Nusselt number with Hartmann number for horizontal and vertical heater at different length at $Ra = 10^6$

It is observed from the figure that the average heat transfer decreases with increasing Hartmann number as the magnetic field effect suppresses the convective recirculating flow within the enclosure. Moreover, decreasing heat transfer rate of vertical heater is faster when compared to horizontal heater of all length.

Figure 12 depicts the behavior of average Nusselt number versus Hartmann number for both horizontal and vertical heaters with $\Gamma = 0.5$ at $Ra = 10^5$, $10^6$ and $10^7$. For all Rayleigh

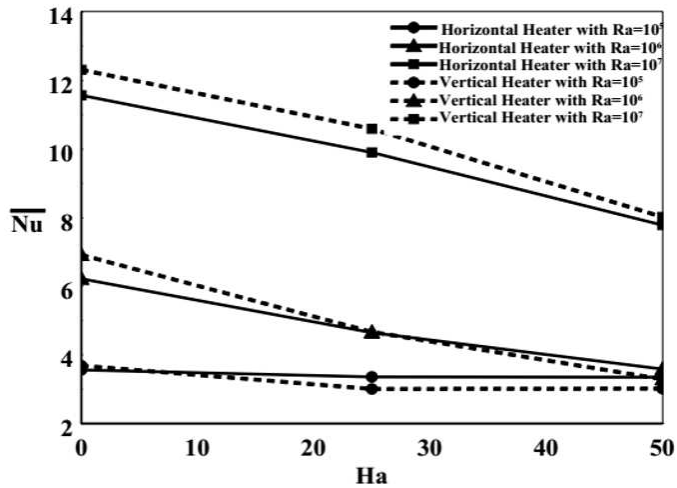


FIGURE 12. Variation of average Nusselt number with Hartmann number for horizontal and vertical heater ($\Gamma = 0.5$) at different Rayleigh numbers

numbers, heat transfer rate decreases as the Hartmann number increases. Moreover, the rate of heat transfer decrease of vertical heater for all Ra values is greater than the horizontal heater.

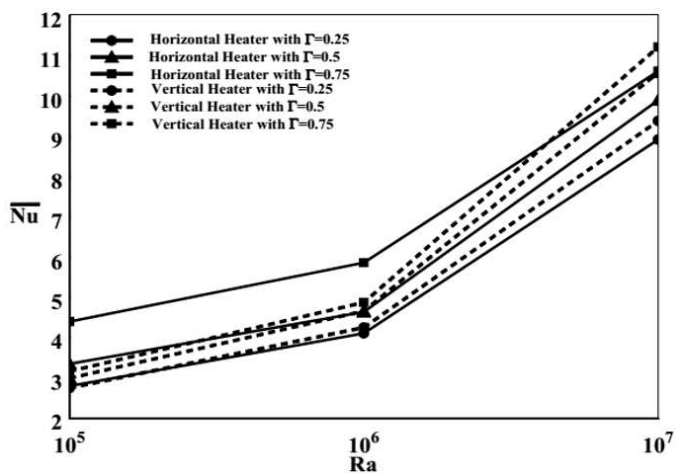


FIGURE 13. Variation of average Nusselt number with Rayleigh number for horizontal and vertical heater of different length at $Ha = 25$

Figure 13 shows the variation of average Nusselt number versus different Rayleigh numbers for both horizontal and vertical heater of different length at $Ha = 25$. It is observed from this

figure that for all Rayleigh numbers, the average Nusselt number increases when the length of heater increases. The effect of different length of vertical heater on heat transfer augmentation is high when compared with horizontal heater. Also the increasing rate of heat transfer for vertical heater of length $\Gamma = 0.75$ attains maximum when compared with rest of all heater with different lengths.

Figure 14 shows the average Nusselt numbers along the vertical walls at various volume fractions of the nanofluid for vertical heater with $\Gamma = 0.75$ at different values of Rayleigh number. It is clearly seen from this figure that the effective thermal conductivity of the nanofluid increases with increasing the volume fraction of the nanoparticles which end results in better heat transfer within the enclosure. So that the high heat transfers for the volume fraction of nanoparticles $\varphi = 0.09$ in the base fluid is obtained for vertical heater of length $\Gamma = 0.75$.

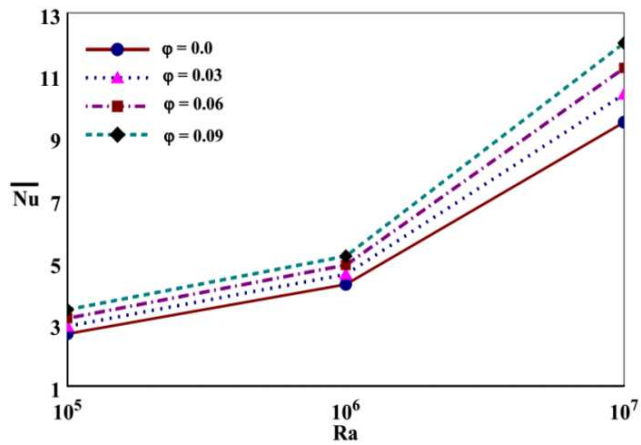


FIGURE 14. Variation of average Nusselt number with Rayleigh number for the enclosure filled with Ag-water nanofluid, vertical heater with length $\Gamma = 0.75$ for different volume fraction of the nanoparticles

## 5. CONCLUSION

The natural convection inside the square enclosure with center heater of different length in the presence of magnetic field has been studied numerically. The present study focuses on the factors that affect the heat transfer. The numerical results obtained can be summarized as follows:

(1) The heat transfer mechanisms and the flow characteristics inside the enclosure depend strongly upon both heater length and strength of magnetic field.
(2) In the absence of the magnetic field, the convection-dominated zone is seen in the enclosure resulting in better convective heat transfer performance for increasing Rayleigh numbers.

(3) Increasing Hartmann number retards the fluid circulation causing lower temperature gradients throughout the enclosure. The convective current in the enclosure is reduced as the Hartmann number increases. Thus for the increasing strength of magnetic field the average Nusselt number decreases.
(4) By adding the nanoparticles to the base fluid heat transfer is augmented and then increased for increasing solid volume fraction of nanoparticles.
(5) Heat transfer enhancement in the enclosure becomes higher for vertically situated center heater than horizontally situated with its maximum length $\Gamma = 0.75$.

## REFERENCES


[1] S. Ostrach, *Natural convection in enclosures*, ASME J. Heat Transfer, **110** (1988) 1175-1190.
[2] H. Turkoglu and N. Yucel, *Effect of heater and cooler locations on natural convection in square cavities*, Numer. Heat Transfer, Part A, **27** (1995) 351-358.
[3] J.H. Bae and J.M. Hyun, *Time-dependent buoyant convection in an enclosure with discrete heat sources*, Int. J. Therm. Sci., **43** (2004) 3-11.
[4] M.A.R. Sharif and T.R. Mohammad, *Natural convection in cavities with constant flux heating at the bottom wall and isothermal cooling from the sidewalls*, Int. J. Therm. Sci., **44** (2005) 865-878.
[5] B. Calcagni, F. Marsili and M. Paroncini, *Natural convective heat transfer in square enclosures heated from below*, Appl. Therm. Eng., **25** (2005) 2522-2531.
[6] A.K. Sharma, K. Velusamy and C. Balaji, *Turbulent natural convection in an enclosure with localized heating from below*, Int. J. Therm. Sci., **46** (2007) 1232-1241.
[7] Y.S. Sun and A.F. Emery, *Effects of wall conduction, internal heat sources and an internal baffle on natural convection heat transfer in a rectangular enclosure*, Int. J. Heat Mass Transfer, **40** (1997) 915-929.
[8] H.F. Oztop, I. Dagtekin and A. Bahloul, *Comparison of position of a heated thin plate located in a cavity for natural convection*, Int. Comm. Heat Mass Transfer, **31** (2004) 121-132.
[9] A. Ben-Nakhi and A.J. Chamkha, *Effect of length and inclination of a thin fin on natural convection in a square enclosure*, Numer. Heat Transfer, Part A, **50** (2006) 381-399.
[10] A.H. Mahmoudi, M. Shahi, A.H. Raouf and A. Ghasemian, *Numerical study of natural convection cooling of horizontal heat source mounted in a square cavity filled with nanofluid*, Int. Commun. Heat Mass Transfer, **37** (2010) 1135-1141.
[11] P. Stefanizzi, A. Lippolis and S. Liuzzi, *Experimental and Numerical Analysis of Heat Transfer in the Cavities of Hollow Blocks*, Int. J. Heat Technology, **31** (2013) 149-154.
[12] S. Jani, M. Mahmoodi, M. Amini and J.E. Jam, *Numerical investigation of natural convection heat transfer in a symmetrically cooled square cavity with a thin fin on its bottom wall*, Therm. Sci., **18** (2014) 1119-1132.
[13] N. Nithyadevi and P. Umadevi, *Natural convection around a heat conducting and generating solid body inside a square enclosure with different thermal boundaries*, J. KSIAM, **19** (2015) 459–479.
[14] Ohk, Seung-Min, Chung and Bum-Jin, *Influence of the Geometry on the Natural Convection Heat Transfer inside a Vertical Cylinder*, Journal of Energy Engineering, **24** (2015) 97-103.
[15] A. Elatar, M.A. Teamah and M.A. Hassab, *Numerical study of laminar natural convection inside square enclosure with single horizontal fin*, Int. J. Therm. Sci., **99** (2016) 41-51.
[16] K. Kalidasan and P. Rajesh Kanna, *Natural convection on an open square cavity containing diagonally placed heaters and adiabatic square block and filled with hybrid nanofluid of nanodiamond - cobalt oxide/water*, Int. Comm. Heat Mass Transfer, **81** (2017) 64-71.
[17] M.H. Esfe, A.A.A. Arani, T. Azizi, S.H. Mousavi and S. Wongwises, *Numerical study of laminar-forced convection of $Al_2O_3$-water nanofluids between two parallel plates*, J. Mech. Sci. Tech., **31** (2017) 785-796.
[18] M. Pirmohammadi and M. Ghassemi, *Effect of magnetic field on convection heat transfer inside a tilted square enclosure*, Int. Commun. Heat Mass Transfer, **36** (2009) 776–780.

[19] D.C. Lo, *High-resolution simulations of magneto hydrodynamic free convection in an enclosure with a transverse magnetic field using a velocity-vorticity formulation*, Int. Commun. Heat Mass Transfer, **37** (2010) 514–523.
[20] G. Saha, *Finite element simulation of magneto convection inside a sinusoidal corrugated enclosure with discrete isoflux heating from below*, Int. Commun. Heat Mass Transfer, **37** (2010) 393–400.
[21] G. Subbarayalu and S.Velappan, *Magneto convection in tilted square cavity with differentially thermally active vertical walls*, J. Math. Statist., **7** (2011) 149–156.
[22] E. Sourtiji and S.F. Hosseinizadeh, *Heat transfer augmentation of magneto hydrodynamics natural convection in L-shaped cavities utilizing nanofluids*, Therm. Sci., **16** (2012) 489–501.
[23] Y. Bakhshan and H. Ashoori, *Analysis of a fluid behavior in a rectangular enclosure under the effect of magnetic field*, Int. J. Mech. Aerospace Eng., **6** (2012) 161–165.
[24] A.M.J. Al-Zamily, *Effect of magnetic field on natural convection in a nanofluid filled semi-circular enclosure with heat flux source*, Comput. Fluids, **103** (2014) 71-85.
[25] M.B. Ben Hamida and K. Charrada, *Natural convection heat transfer in an enclosure filled with an ethylene glycol-copper nanofluid under magnetic fields*, Numer. Heat Transfer, **67** (2015) 902-920.
[26] K. Javaherdeh, M. Moslemi and M. Shahbazi, *Natural convection of nanofluid in a wavy cavity in the presence of magnetic field on variable heat surface temperature*, J. Mech. Sci. Tech., **31** (2017) 1937-1945.
[27] A.K. Santra, S. Sen and N. Chakraborty, *Study of heat transfer augmentation in a differentially heated square cavity using copper water nanofluid*, Int. J. Therm. Sci., **47** (2008) 1113-1122.
[28] C.J. Ho, M.W. Chen and Z.W. Li, *Numerical simulation of natural convection of nanofluid in a square enclosure: effects due to uncertainties of viscosity and thermal conductivity*, Int. J. Heat Mass Transfer, **51** (2008) 4506-4516.
[29] H.F. Oztop and E. Abu-Nada, *Numerical study of natural convection in partially heated rectangular enclosures filled with nanofluids*, Int. J. Heat Fluid Flow, **29** (2008) 1326-1336.
[30] S.M. Aminossadati and B. Ghasemi, *Natural convection cooling of a localized heat source at the bottom of a nanofluid-filled enclosure*, Eur. J. Mech. B/Fluids, **28** (2009) 630-640.
[31] E. Abu-nada and H. Oztop, *Effect of inclination angle on natural convection in enclosures filled with Cu-Water nanofluid*, Int. J. Heat Fluid Flow, **30** (2009) 669-678.
[32] E.B. Ogut, *Natural convection of water-based nanofluids in an inclined enclosure with a heat source*, Int. J. Therm. Sci., **48** (2009) 2063-2073.
[33] E. Abu-nada, Z. Masoud and H. Oztop, A. Campo, *Effect of nanofluid variable properties on natural convection in enclosures*, Int. J. Therm. Sci., **49** (2010) 479-491.
[34] B. Ghasemi, S.M. Aminossadati and A. Raisi, *Magnetic field effect on natural convection in a nanofluid-filled square enclosure*, Int. J. Thermal Sciences, **50** (2011) 1748-1756.
[35] M. Sheikholeslami and M. Gorji-Banpy, *Free convection of ferrofluid in a cavity heated from below in the presence of an external magnetic field*, Powder technology, **256** (2014) 490-498.
[36] F. Selimefendigil, H.F. Oztop and N. Abu-Hamdeh, *Natural convection and entropy generation in nanofluid filled entrapped trapezoidal cavities under the influence of magnetic field*, Entropy, **18** (2016) 1-22.
[37] S.V. Patankar, *Numerical heat transfer and fluid flow, Hemisphere Publishing Corporation*, USA, 2004.
[38] M. Mahmoodi, *Numerical simulation of free convection of nanofluid in a square cavity with an inside heater*, Int. J. Therm. Sci., **50** (2011) 2161-2175.